

Kinetic Alfvén wave instability in a Lorentzian dusty magnetoplasma

Cite as: Phys. Plasmas **17**, 103704 (2010); <https://doi.org/10.1063/1.3491336>

Submitted: 02 August 2010 . Accepted: 24 August 2010 . Published Online: 18 October 2010

N. Rubab, N. V. Erkaev, D. Langmayr, and H. K. Biernat



View Online



Export Citation

ARTICLES YOU MAY BE INTERESTED IN

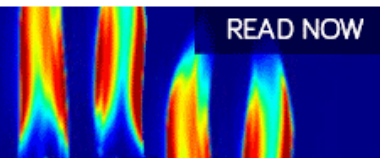
[Kinetic Alfvén wave instability in a Lorentzian dusty plasma: Non-resonant particle approach](#)
Physics of Plasmas **18**, 073701 (2011); <https://doi.org/10.1063/1.3599600>

[Dust kinetic Alfvén and acoustic waves in a Lorentzian plasma](#)
Physics of Plasmas **16**, 103704 (2009); <https://doi.org/10.1063/1.3244625>

[Dust kinetic Alfvén waves and streaming instability in a non-Maxwellian magnetoplasma](#)
Physics of Plasmas **21**, 063702 (2014); <https://doi.org/10.1063/1.4879803>

AIP Advances
Fluids and Plasmas Collection

READ NOW



Kinetic Alfvén wave instability in a Lorentzian dusty magnetoplasma

N. Rubab,¹ N. V. Erkaev,² D. Langmayr,³ and H. K. Biernat¹

¹Space Research Institute, Austrian Academy of Sciences, Schmiedlstrasse 6, A-8042 Graz, Austria
and Institute of Physics, University of Graz, Universitätsplatz 5, A-8010 Graz, Austria

²Institute of Computational Modelling, 660036 Krasnoyarsk, Russia
and Siberian Federal University, 660041 Krasnoyarsk, Russia

³Virtual Vehicle Competence Center (vif), Inffeldgasse 21a, 8010 Graz, Austria

(Received 2 August 2010; accepted 24 August 2010; published online 18 October 2010)

This study presents a theoretical approach to analyze the influence of kappa distributed streaming ions and magnetized electrons on the plasma wave propagation in the presence of dust by employing two-potential theory. In particular, analytical expressions under certain conditions are derived for various modes of propagation comprising of kinetic Alfvén wave streaming instability, two stream instability, and dust acoustic and whistler waves. A dispersion relation for kinetic Alfvén-like streaming instability has been derived. The effects of dust particles and Lorentzian index on the growth rates and the threshold streaming velocity for the excitation of the instability are examined. The streaming velocity is observed to be destabilizing for slow motion and stabilizing for fast streaming motions. It is also observed that the presence of magnetic field and superthermal particles hinders the growth rate of instability. Possible applications to various space and astrophysical situations are discussed. © 2010 American Institute of Physics. [doi:10.1063/1.3491336]

I. INTRODUCTION

When two clouds of plasma merge into each other, certain disturbances in the electromagnetic field will tend to grow. The phenomena that cause it are called beam plasma instabilities. The particle beam creates a reverse current in the target plasma to end up with a classical two stream instability. These instabilities release the excess of free energy stored in the particle streaming which can excite different plasma modes. Recently, there has been much interest in studying purely growing electrostatic/electromagnetic instabilities driven by the streaming of plasma particles relative to each other.¹⁻⁷ A number of electromagnetic instabilities have been studied, which are mainly triggered by ion beams parallel to the magnetic field.⁸ To study such instabilities in dusty plasmas is quite different from electron-ion plasmas as the presence of massive dust grains contribute to the growth and damping of the instabilities and introduce new types of waves, which appear on new time and space scales.⁹ Such type of instabilities in an unmagnetized dusty plasma have been investigated by a number of authors to show the excitation/decay due to the effect of particle dynamics.¹⁰⁻¹² Magnetized dusty plasmas support additional electrostatic low frequency waves involving the dynamics of magnetized/unmagnetized dust grains and magnetized electrons/ions. One of these waves is the dust lower hybrid (DLH) wave with $\omega \ll \omega_{ci}$, which propagates nearly perpendicular to the external magnetic field.^{13,14} This mode basically arises due to unmagnetized dust and magnetized lighter plasma particles. It has been shown theoretically that in a streaming magnetized plasma, the velocity of ions is coupled directly with DLH and dust acoustic modes.¹⁵ Through this coupling, the low-phase velocity wave can take the particle streaming energy, and due to the gain of energy, the amplitude of the mode will tend to grow.

The relative streaming of plasma components along an external magnetic field at speeds greater than the Alfvén speed can excite numerous instabilities. Most of them have the largest growth rates with a propagation vector along the magnetic field direction.¹⁶ The damping/excitation and propagation of Alfvén waves could be affected by the presence of dust and modify the behavior of these low frequency waves in a dusty plasma.¹⁷ An extensive study has been carried out to study the unstable wave modes in the circularly polarized branch driven in the solar wind by the Martian heavy ion beam.¹⁸ The instability of circularly polarized Alfvén waves in plasmas with proton beams and the coupling effects through hybrid simulations have been studied most recently.¹⁹ The dust grains were exempted in both above mentioned studies. However, it has been recently recognized that in the presence of dust particles, the characteristics of circularly polarized Alfvén waves are modified and several couplings between distinct branches of the dispersion relation appear.^{20,21} Further, it is shown that the growth rate of instability can be affected by the presence of dust grains.²² A kinetic formulation to analyze Alfvén wave propagation in the presence of inelastic dust charge fluctuations has also been developed.²³

In most of these theoretical investigations reported so far, the particle distribution has been assumed to be Maxwellian. Space-craft measurements of electron energy spectra and *in situ* observations in the near-Earth space plasma clearly indicate the presence of superthermal particle populations. These particles may arise due to the effect of external forces acting on the natural space environments or due to wave-particle interaction. The observed distribution contains a plentiful supply of superthermal particles, i.e., particles that move faster than the thermal speed and are represented by the family of kappa distribution. These populations are modeled with the so-called kappa distribution function which

obeys a power law in particle speed with high energy tails and, for large values of kappa ($\kappa \rightarrow \infty$), degenerates into its Maxwellian counterpart. Such deviations from Maxwellian distributions are expected to exist in a low density plasma where binary collisions are sufficiently rare. The presence of high energy tail component in a kappa distribution effectively changes the rate of resonant energy transfer between particles and plasma waves and therefore, it is expected that the conditions for instability may be different from the Maxwellian counterpart.²⁴ The occurrence of kappa distribution is attributed to the wave-particle interactions which are responsible for the particle energization. For instance, such distributions have been used to analyze the low energy electrons in the Earth's magnetosphere,^{25,26} Alfvén waves in solar wind streams,²⁷ and whistler emission of Jupiter.²⁸ Much of the work has been devoted to study electron/ion plasma without considering the effects of dust grains. Recently, some new models for nonthermal plasmas [such as (r, q) distribution] have been employed to study various electrostatic and electromagnetic waves and instabilities in a dusty/dust free plasmas.^{29–34}

Kinetic Alfvén wave (KAW) like streaming instabilities in a dusty plasma using a two-potential approach have not been investigated, when the background plasma is kappa distributed. Our aim is to fill in the gap and highlight the influence of kappa distributed ions and unmagnetized dust on the streaming instabilities.

The layout of this manuscript is organized as follows. Basic assumptions and equations leading toward the general form of the dispersion relation for streaming instabilities in terms of the modified Lorentzian plasma dispersion function is discussed in Secs. II–IV. Results and conclusions are discussed in Secs. V and VI, respectively.

II. BASIC ASSUMPTIONS

We consider an electromagnetic KAW-like streaming instability in a collisionless electron-ion dusty magnetoplasma. We assume strongly magnetized electrons to be Maxwellian and a beam of kappa distributed ions flowing along an external magnetic field ($\mathbf{B}_0 \parallel \hat{z}$) with constant ion drift velocity ($V_0 \parallel \mathbf{B}_0$), while dust is cold and unmagnetized. The plasma beta β_i is assumed to be very small, i.e., $\beta_i \ll 1$, where $\beta_i = 4\pi n_{i0} T_i / B_0^2$. The electric field and the wave vector \mathbf{k} lie in the xz plane. Thus we have

$$\mathbf{B}_0 = \begin{pmatrix} 0 \\ 0 \\ B_0 \end{pmatrix}, \quad \mathbf{V}_0 = \begin{pmatrix} 0 \\ 0 \\ V_0 \end{pmatrix}, \quad \mathbf{k} = \begin{pmatrix} k_\perp \\ 0 \\ k_\parallel \end{pmatrix}.$$

For a low beta plasma, we may neglect the electromagnetic wave compression along the direction of the external magnetic field ($B_{1z} = 0$). Therefore, the choice of a particular coordinate system allows us to make use of two-potential theory by assuming two different electrostatic potentials to represent the transverse and parallel component of electric field, i.e.,

$$E_\perp = -\nabla_\perp \varphi,$$

$$E_\parallel = -\frac{\partial \psi}{\partial z},$$

where $\varphi \neq \psi$.

The linearized Poisson equation is

$$\nabla_\perp^2 \varphi + \frac{\partial^2 \psi}{\partial z^2} = 4\pi e \left[n_{e1} - n_{i1} - \frac{Q_{d0}}{e} n_{d1} - \frac{n_{d0}}{e} Q_{d1} \right], \quad (1)$$

where n_{e1} , n_{i1} , and n_{d1} are electron, ion, and dust number densities, respectively, $Q_{d0} = -Z_d e$ (with Z_d as the number of electron charge on a grain) is the equilibrium charge on an average dust grain, and e is the electron charge. Here, we consider negatively charged dust grains which are charged by electron currents.

We ignore the dust charge fluctuation effects, i.e., $Q_{d1} = 0$, as the dust charge fluctuation causes a non-Landau-type damping, known as Tromsø damping, which is usually important for low frequency electrostatic waves involving the dynamics of dust grains.^{35,11}

Combining Ampere's and Faraday's laws, we get,³⁶

$$\frac{\partial}{\partial z} \nabla_\perp^2 (\varphi - \psi) = \frac{4\pi}{c^2} \frac{\partial}{\partial t} [J_{e1z} + J_{i1z} + J_{d1z}], \quad (2)$$

where the J 's are the field aligned current densities.

The perturbed distribution function of ions is given by the aid of Vlasov equation

$$f_{i1} = -\frac{ek_\parallel \psi}{m_i (\omega - k_\parallel v_\parallel)} \frac{\partial f_{i0}^\kappa}{\partial v_\parallel}, \quad (3)$$

where f_{i0}^κ is the zeroth order distribution function and is assumed to obey a power law form,⁵ i.e.,

$$f_{i0}^\kappa = A_{i\kappa} \left\{ 1 + \frac{1}{\kappa v_{i\kappa}^2} [v_\perp^2 + (v_\parallel - V_0)^2] \right\}^{-\kappa-1}, \quad (4)$$

where

$$A_{i\kappa} = n_{i0} \left(\frac{1}{\pi \kappa v_{i\kappa}^2} \right)^{3/2} \frac{\Gamma(\kappa + 1)}{\Gamma(\kappa - 1/2)}; \quad \kappa > 3/2$$

and

$$v_{i\kappa}^2 = \left(\frac{2\kappa - 3}{\kappa} \right) \left(\frac{T_i}{m_i} \right),$$

where κ is the spectral index, Γ is the Gamma function, and thermal speed $v_{i\kappa}$ is related to the particle temperature T_i .

Important features associated with a κ distribution are that it tends to a Maxwellian distribution for the limit $\kappa \rightarrow \infty$, obeys an inverse power form for high velocities, and allows one to model superthermal particle contributions within the plasma.

We solve the Vlasov equation for hot and magnetized electrons in terms of the guiding center coordinates and get the perturbed distribution for any electromagnetic wave,^{37,38}

$$f_{e1} = - \left(\frac{n_{e0} e}{T_e} \right) \sum_l \sum_n \frac{k_{\parallel} v_{\parallel} \psi + n \Omega_{ce} \varphi}{\omega - n \Omega_{ce} - k_{\parallel} v_{\parallel}} \times \exp[i(n-l)\theta] J_n \left(\frac{k_{\perp} v_{\perp}}{\Omega_{ce}} \right) J_l \left(\frac{k_{\perp} v_{\perp}}{\Omega_{ce}} \right) f_{e0}, \quad (5)$$

where f_{e0} is the equilibrium Maxwellian distribution function for electrons and Ω_{ce} is the electron cyclotron frequency.

The dust component is considered to be cold and unmagnetized and thus, we use a hydrodynamical approach for finding the dust number density and current density.

III. NUMBER DENSITY AND CURRENT DENSITY PERTURBATIONS

Making use of Eqs. (3) and (4), we get the perturbed number density of Lorentzian type streaming ions

$$n_{i1} = - \frac{2en_{i0}\psi}{m_i v_{ii\kappa}^2} \left[\frac{2\kappa - 1}{2\kappa} + \eta Z(\eta) \right], \quad (6)$$

where

$$\eta = \frac{\omega - k_{\parallel} V_0}{k_{\parallel} v_{ii\kappa}} \quad (7)$$

and

$$Z(\eta) = \frac{1}{\pi^{1/2}} \frac{\Gamma(\kappa + 1)}{\kappa^{3/2} \Gamma(\kappa - 1/2)} \int_{-\infty}^{+\infty} \frac{x dx}{(x - \eta)(1 + x^2/\kappa)^{\kappa+1}}$$

is the Lorentzian type plasma dispersion function.³⁹

The number density of hot and magnetized electrons can be written as

$$n_{e1} = \frac{2en_{e0}\psi}{k_{\parallel} m_e v_{te}^2} \sum_n \{ k_{\parallel} v_{te} \psi [1 + \xi_{en} Z(\xi_{en})] + n \Omega_{ce} \varphi Z(\xi_{en}) \} I_n(b_e) e^{-b_e}, \quad (8)$$

where I_n is the modified Bessel function with argument $b_e = k_{\perp}^2 v_{te}^2 / 2\omega_{ce}^2$ and $Z(\xi_{en})$ is the usual dispersion function for a Maxwellian plasma with

$$\xi_{en} = \frac{\omega - n \Omega_{ce}}{k_{\parallel} v_{te}}.$$

The perturbed number density of cold and unmagnetized dust grains is given by the momentum balance and continuity equations

$$n_{d1} = \frac{n_{d0} Q_{d0}}{m_d \omega^2} (k_{\perp}^2 \varphi + k_{\parallel}^2 \psi). \quad (9)$$

The longitudinal components of current density perturbations are given by^{36,40,41}

$$J_{i1z} = - \frac{2e^2 n_{i0} \psi}{m_i v_{ii\kappa}} \left[\frac{2\kappa - 1}{2\kappa} \eta + \eta^2 Z(\eta) \right], \quad (10)$$

$$J_{e1z} = - \frac{n_{e0} e^2}{T_e k_{\parallel}} \sum_n \{ [1 + \xi_{en} Z(\xi_{en})] \times (k_{\parallel} v_{te} \xi_{en} \psi + n \Omega_{ce} \varphi) \} I_n(b_e) e^{-b_e}, \quad (11)$$

and

$$J_{d1z} = \frac{n_{d0} Q_{d0}^2}{m_d \omega} k_{\parallel} \psi. \quad (12)$$

IV. DISPERSION RELATION

Now, using the explicit expressions of n_{e1} , n_{i1} , and n_{d1} in Eq. (1) and J_{i1z} , J_{e1z} , and J_{d1z} in Eq. (2) allows to obtain the following system of equations:

$$A\varphi + B\psi = 0, \quad (13)$$

$$C\varphi + D\psi = 0,$$

where

$$A = k_{\perp}^2 + \frac{2\omega_{pe}^2}{v_{te}^2} \left[\frac{n \Omega_{ce}}{k_{\parallel} v_{te}} Z(\xi_{en}) I_n e^{-b_e} \right] - k_{\perp}^2 \frac{\omega_{pd}^2}{\omega^2},$$

$$B = k_{\parallel}^2 + \frac{2\omega_{pi}^2}{v_{ii\kappa}^2} \left[\frac{2\kappa - 1}{2\kappa} + \eta Z(\eta) \right] + \frac{2\omega_{pe}^2}{v_{te}^2} [1 + \xi_{en} Z(\xi_{en})] I_n e^{-b_e} - k_{\parallel}^2 \frac{\omega_{pd}^2}{\omega^2}, \quad (14)$$

$$C = c^2 k_{\parallel} k_{\perp}^2 + \frac{\omega_{pe}^2 n \omega \Omega_{ce}}{v_{te}^2 k_{\parallel}} [1 + \xi_{en} Z(\xi_{en})] I_n e^{-b_e},$$

$$D = \frac{2\omega_{pi}^2}{v_{ii\kappa}} \eta \left[\frac{2\kappa - 1}{2\kappa} + \eta Z(\eta) \right] - k_{\parallel} (k_{\perp}^2 c^2 + \omega_{pd}^2).$$

The dispersion relation is obtained by solving the homogeneous equation (13), i.e.,

$$AD - BC = 0. \quad (15)$$

Substituting the values of A, B, C, D from Eq. (14) and after a straightforward algebra, we get

$$1 + \frac{2\omega_{pe}^2}{k_{\parallel}^2 v_{te}^2} \sum_n \left\{ \left(1 + \frac{\omega_{pd}^2}{k_{\perp}^2 c^2} \right) \frac{n \Omega_{ce}}{k_{\parallel} v_{te}} Z(\xi_{en}) I_n e^{-b_e} + \left(1 - \frac{\omega v_{te} \xi_{en}}{c^2 k_{\parallel}} + \frac{n \omega \Omega_{ce}}{k_{\perp}^2 c^2} \right) [1 + \xi_{en} Z(\xi_{en})] I_n e^{-b_e} \right\} + \frac{2\omega_{pi}^2}{k_{\parallel}^2 v_{ii\kappa}^2} \left\{ \left(1 - \frac{2v_{ii\kappa} \omega \eta}{c^2 k_{\parallel}} \right) \left(1 - \frac{\omega_{pd}^2}{\omega^2} \right) \times \left[\frac{\kappa - 1/2}{\kappa} + \eta Z(\eta) \right] \right\} + \frac{\omega_{pd}^2}{k_{\parallel}^2 c^2} + \frac{k_{\perp}^2}{k_{\parallel}^2} - \left(1 + \frac{k_{\perp}^2}{k_{\parallel}^2} \right) \frac{\omega_{pd}^2}{\omega^2} = 0, \quad (16)$$

which is the dispersion relation of kinetic Alfvén-like streaming instabilities in a Lorentzian dusty plasma. One can immediately notice the effect of nonthermality via the kappa-

modified plasma dispersion function and dust effects (which will give rise to the dust lower hybrid frequency) on the dispersion characteristics.

Several classical wave modes can be derived from the above dispersion equation by the consideration of particular limits. For a clear overview, we consider two special cases, i.e.,

(i) ($\mathbf{k} \parallel \mathbf{B}_0, V_0$).

We investigate the wave propagation along the magnetic field and streaming direction, i.e., along the z -axis. The particles can stream freely along the magnetic field directions, while their motion in the perpendicular direction is suppressed by the gyromotion of plasma particles; therefore, this is the most plausible case.

Under these assumptions, along with $n=0$ and $b_e \ll 1$, Eq. (16) could be visualized as the two stream electrostatic instability in a dusty plasma

$$1 + \frac{2\omega_{pe}^2}{k_{\parallel}^2 v_{te}^2} [1 + \zeta_{en} Z(\zeta_{en})] + \frac{2\omega_{pi}^2}{k_{\parallel}^2 v_{ii\kappa}^2} \left[\frac{\kappa - 1/2}{\kappa} + \eta Z(\eta) \right] - \frac{\omega_{pd}^2}{\omega^2} = 0. \quad (17)$$

It is clear that the electrostatic dispersion relation for waves parallel to the magnetic field is identical to the familiar electrostatic dispersion relation for an unmagnetized plasma. Since the wave vector \mathbf{k} is parallel to \mathbf{B}_0 , the electrostatic stability properties are unaffected by the presence of the magnetic field.

Such type of results have been found for a dust free plasma.⁴² The fluid version of the above equation for different streaming species illustrate that the presence of dust enhances the growth rate of instability.¹⁷ In the limit $\kappa \rightarrow \infty$, $\omega_{pd}^2 = 0$, our results approaches to its classical Maxwellian counterpart.⁴³

(ii) ($\mathbf{k} \parallel \mathbf{B}_0$), $V_0 = 0$, ($\omega_{ci} \ll \omega \ll \Omega_{ce}$).

By expanding the plasma dispersion function and ignoring the effect of dust in Eq. (16), we get whistler like mode whose frequency is below the electron cyclotron frequency. After some straightforward calculations, we get

$$\omega = \frac{c^2 k_{\parallel} \Omega_{ce}}{\omega_{pe}^2}, \quad (18)$$

where c^2/ω_{pe}^2 is the electron skin depth and

$$v_{ph} = \frac{c^2 k_{\parallel} \Omega_{ce}}{\omega_{pe}^2},$$

which shows that the phase velocity of whistler waves is unaffected by the form of the distribution function.

Now, by applying suitable approximations $\omega \ll \omega_{ce}, b_e \ll 1$ and expanding the plasma dispersion function, Eq. (16) turns out to be

$$A = \frac{k_{\perp}^2}{\omega^2} f_e (\omega^2 - \omega_{DLH}^2),$$

$$B = \frac{1}{\lambda_{Di\kappa}^2} - k_{\parallel}^2 \frac{\omega_{pd}^2}{\omega^2}, \quad (19)$$

$$C = k_{\parallel} k_{\perp}^2 c^2,$$

$$D = \left(\frac{2\kappa - 1}{\kappa} \right) \omega \frac{\omega_{pi}^2}{k_{\parallel} v_{ii\kappa}^2} (\omega - k_{\parallel} V_0) - k_{\parallel} (k_{\perp}^2 c^2 + \omega_{pd}^2),$$

where $\omega_{DLH}^2 = (\omega_{pd}^2 \Omega_{ce}^2) / \omega_{pe}^2$, $f_e = \omega_{pe}^2 / \Omega_{ce}^2$, and $\lambda_{Di\kappa} = \sqrt{T_i / 4\pi n_{i0} e^2 (\kappa - 3/2 / \kappa - 1/2)}$.

Now, making use of Eq. (15), we arrive at

$$(\omega^2 - \omega_{DLH}^2) \left[\left(\frac{2\kappa - 1}{\kappa} \right) \frac{\omega_{pi}^2}{k_{\parallel} v_{ii\kappa}^2} (\omega^2 - \omega k_{\parallel} V_0) - k_{\parallel} \times (k_{\perp}^2 c^2 + \omega_{pd}^2) \right] - \frac{k_{\parallel} V_{Ae}^2}{\lambda_{Di\kappa}^2} [\omega^2 - k_{\parallel}^2 \omega_{pd}^2 \lambda_{Di\kappa}^2] = 0, \quad (20)$$

where $V_{Ae} = B_0 / (4\pi n_{e0} m_e)^{1/2}$ is the electron Alfvén speed with electron mass density.⁴⁴ This equation shows that due to the thermal kinetic effect, the shear Alfvén wave develops a longitudinal component, making a kinetic Alfvén wave a mixed electromagnetic and electrostatic mode. It also shows that dusty plasma supports dust lower hybrid waves due to nearly perpendicular propagation and dust acoustic wave (DAW) due to nearly parallel propagation.

In the limit $\omega^2 / k_{\parallel}^2 V_A^2 \rightarrow 0$, $V_0 = 0$, and $k_{\perp}^2 \rho_e^2 \ll 1$, we get

$$\omega^2 = \left(\frac{2\kappa - 3}{2\kappa - 1} \right) k_{\parallel}^2 C_D^2, \quad (21)$$

where $C_D^2 = Z_{d0} T_i / m_d$.

This equation is the dispersion relation for the dust acoustic wave in a Lorentzian plasma. In the limit $\kappa \rightarrow \infty$, we approach a Maxwellian DAW.⁴⁵

After simplifying Eq. (20), we will get a quartic equation, i.e.,

$$a\omega^4 + b\omega^3 + c\omega^2 + d\omega + e = 0, \quad (22)$$

which is the dispersion relation for kinetic Alfvén wave instabilities, where

$$a = 1,$$

$$b = -k_{\parallel} V_0,$$

$$c = -\omega_{DLH}^2 - k_{\parallel}^2 V_{Ae}^2 - k_{\parallel}^2 \lambda_{Di\kappa}^2 (k_{\perp}^2 c^2 + \omega_{pd}^2),$$

$$d = \omega_{DLH}^2 k_{\parallel} V_0,$$

$$e = k_{\parallel}^2 \omega_{DLH}^2 \lambda_{Di\kappa}^2 (k_{\perp}^2 c^2 + \omega_{pd}^2) + k_{\parallel}^4 V_{Ae}^2 \omega_{pd}^2 \lambda_{Di\kappa}^2,$$

for $V_0 = 0$, $b = d = 0$, and we will get a kinetic Alfvén-like wave

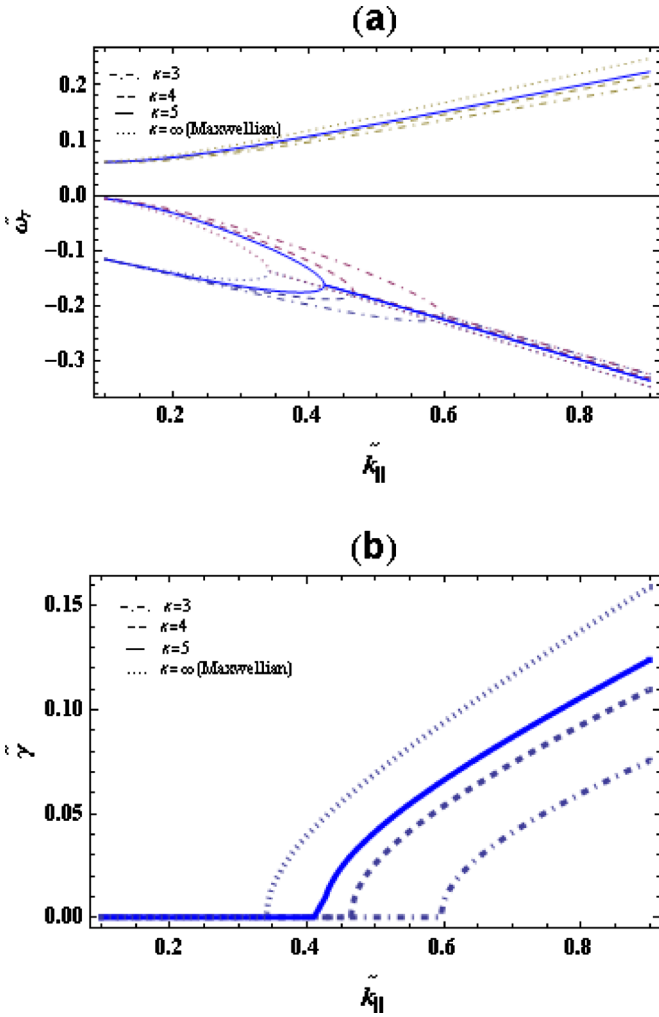


FIG. 1. (Color online) Effect of κ on the real ($\tilde{\omega}_r$) and imaginary ($\tilde{\gamma}$) parts of the dispersion relation for $\tilde{V}_0=1.5$ and $\beta_i=0.1$.

$$\omega^2 = \omega_{\text{DLH}}^2 + k_{\parallel}^2 V_{Ae}^2 \left[1 + \left(\frac{2\kappa - 3}{2\kappa - 1} \right) \delta_e \left(1 + \frac{\omega_{pd}^2}{c^2 k_{\perp}^2} \right) k_{\perp}^2 \rho_e^2 \right], \quad (23)$$

where $\rho_e^2 = T_i/m_e \Omega_{ce}^2$, $\delta_e = n_{e0}/n_{i0}$, and $V_{Ae} = c\Omega_{ce}/\omega_{pe}$.

This dispersion relation shows that the kinetic Alfvén waves and dust acoustic modes are coupled. The two modes decouple for $\beta_i \ll 1$, i.e., the coupling between kinetic Alfvén wave and the dust acoustic wave becomes weak.

Since $k_{\perp}^2 \rho_e^2 \ll 1$, we can ignore the third term on the right hand side and ultimately, we get

$$\omega^2 = \omega_{\text{DLH}}^2 \left(1 + \frac{k_{\parallel}^2 c^2}{\omega_{pd}^2} \right), \quad (24)$$

where $\omega_{\text{DLH}}^2 = \omega_{pd}^2 \Omega_{ce}^2 / \omega_{pe}^2$ is the dust lower hybrid frequency which arises due to the hybrid motion of magnetized electrons and unmagnetized dust grains. The unmagnetized dust introduces ω_{DLH}^2 , a new cutoff frequency which gives rise to a limit for the propagation of electromagnetic waves in a dusty plasma.

In the opposite case, when the streaming electrons follow kappa distribution and ions are magnetized, the low fre-

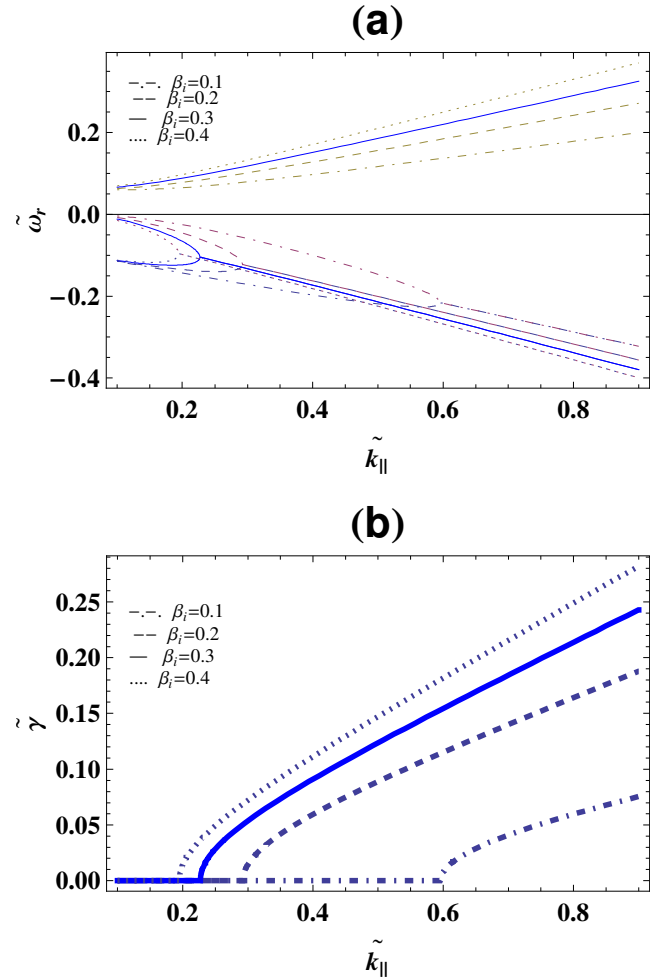


FIG. 2. (Color online) Effect of β_i on the real ($\tilde{\omega}_r$) and imaginary ($\tilde{\gamma}$) parts of the dispersion relation for $\tilde{V}_0=1.5$ and $\kappa=3$.

quency ion fluctuations couple with the Doppler-shifted electron plasma oscillations in the beam. For $V_{0e} > \omega/k_{\parallel}$, we get the kinetic Alfvén wave instability below ion cyclotron frequency.

V. RESULTS

Now, we discuss the solution of Eq. (22) for several parameters which are close to dusty plasma environments in interstellar clouds.^{46–48} Interstellar dust make up only 1% of the interstellar medium but sometimes there is enough dust to obscure the light from stars behind the dust. The interstellar medium contains carbon, helium, hydrogen, and other gases such as oxygen, nitrogen, and baryonic gas molecules. In order to study waves and instabilities in interstellar molecular clouds, one must consider the effect of heavy dust particles as a component of neutral fluid. We do not choose a particular example of dust species as our aim is to show how the presence of dust grains affects the electromagnetic instability. Here, we consider $n_{i0} = 10-10^4 \text{ cm}^{-3}$, $n_{d0} = 10-10^{-2} \text{ cm}^{-3}$, $Z_d = 10-10^4$, $m_d = 10^5-10^8 m_i$.

For computational convenience, we introduce dimensionless parameters as follows:

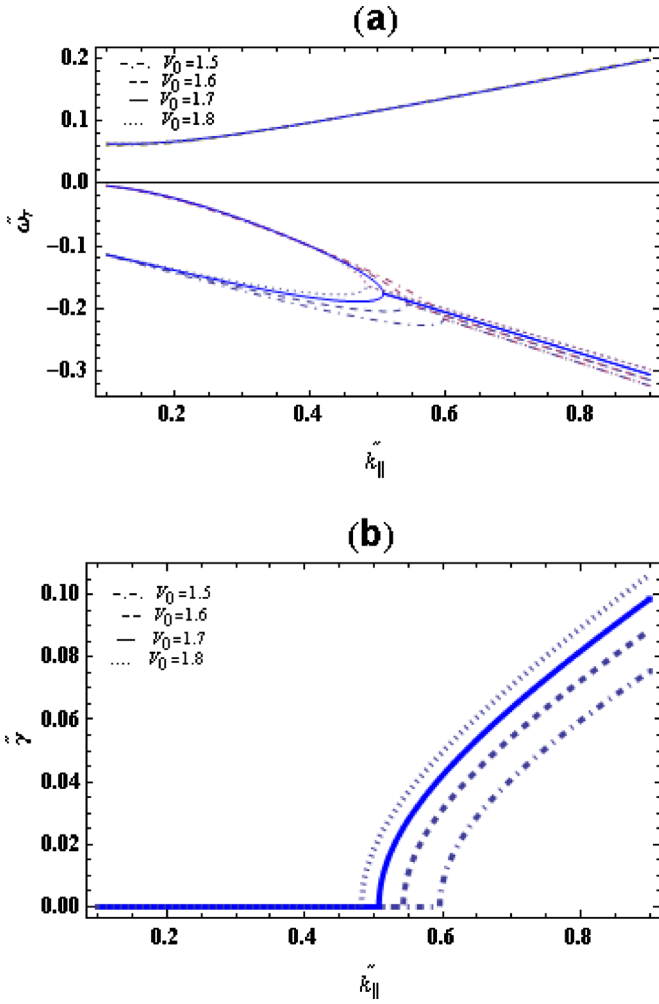


FIG. 3. (Color online) Effect of \tilde{V}_0 on the real ($\tilde{\omega}_r$) and imaginary ($\tilde{\gamma}$) parts of the dispersion relation for $\beta_i=0.1$ and $\kappa=3$.

$$\omega = \Omega_{ce}\tilde{\omega}, \quad k_{\parallel} = \frac{\Omega_{ce}}{V_A}\tilde{k}_{\parallel}, \quad V_0 = V_A\tilde{V}_0.$$

The dispersion relation (20) shows that kinetic Alfvén waves and dust acoustic modes are coupled. For $\beta_i \ll 1$, the coupling between the dust acoustic and kinetic Alfvén wave becomes weak and the two modes decouple, leading to the dispersion relation for the kinetic Alfvén and dust acoustic modes. It is shown here that the ion beam with streaming velocity V_0 , passing through a background plasma, may act as an effective source of low frequency wave excitation. The effects of different parameters on kinetic Alfvén-like streaming instability (stability) are shown in Figs. 1–4, when k_{\perp} is held constant. Each mode in Eq. (20) has two branches corresponding to plus and minus signs in the dispersion equation and the negative value of ω corresponds to a backward propagating wave with respect to the z -axis. The upper branch shows the kinetic Alfvén wave, while the lower frequency branch is near to the cutoff frequency ω_{DLH} , which is excited due to κ -distributed ion beam source as shown in the (a) panels of Figs. 1–4. Lower instability is caused by the interaction between the ion beam and KAW near ω_{DLH} ,

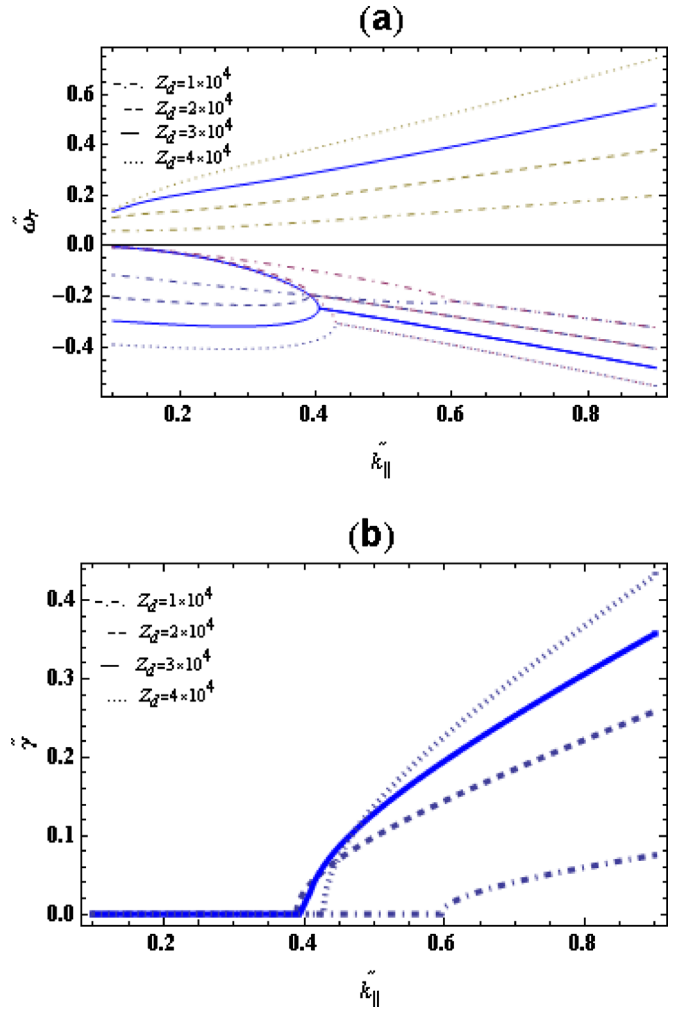


FIG. 4. (Color online) Effect of Z_d on the real ($\tilde{\omega}_r$) and imaginary ($\tilde{\gamma}$) parts of the dispersion relation for $\beta_i=0.1$, $\kappa=3$, and $\tilde{V}_0=1.5$.

which is shown in the (b) panels of Figs. 1–4 for different plasma parameters.

The real frequency of the kinetic Alfvén waves decreases for lower values of κ , while it becomes maximum for a Maxwellian plasma, as shown in Fig. 1(a). Similarly, for low values of κ , the instability reduces, while increasing the value of Lorentzian index the amplitude of unstable region increases, and for $\kappa \rightarrow \infty$ (Maxwellian), we get maximum growth rate, as shown in Fig. 1(b). The instability region is restricted to a critical value of \tilde{k}_{\parallel} , the so-called cutoff wave number, which limits the instability to grow beyond this value. For $k_{\parallel} \leq 0.34$, we have a stable region for a Maxwellian plasma while for $\kappa=3$, the stable region increases toward large \tilde{k}_{\parallel} . Through coupling, the waves exchange energy and increase the level of instability. It is also important to note that maximum growth rate occurs for small wave number and vice versa. In short, the unstable region is limited to $0.6 \gg \tilde{k}_{\parallel} \gg 0.34$.

In Fig. 2(a), $\tilde{\omega}_r$ is shown as a function of \tilde{k}_{\parallel} for various values of plasma β_i and κ remains fixed at $\kappa=3$. Figure 2(b) shows that on varying β_i , we can observe prominent increment in the growth rate of instability. The stable region di-

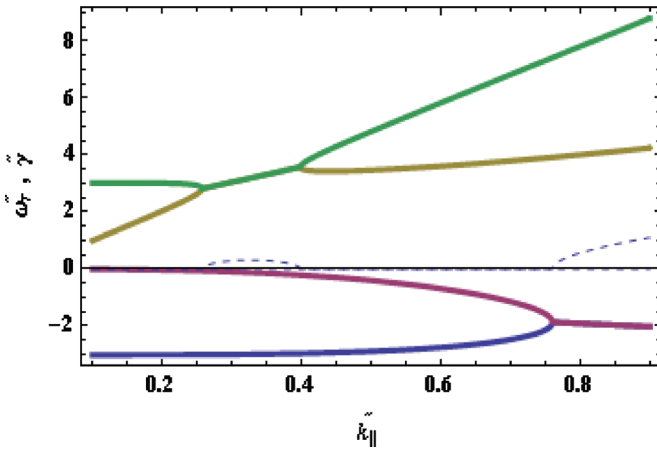


FIG. 5. (Color) Real (solid lines) and imaginary (dashed lines) plots of the dispersion relation for $n_{d0} > 10^{-2}$, $\tilde{V}_0 = 10$, and $\beta_i = 0.5$.

minishes for large values of β_i , which shows that a strong magnetic field helps to stabilize the system. It is observed that the superthermal particles with a weak magnetic field enhance the growth rates. The growth rates are increased toward small wave numbers.

The effects of ions streaming on the real and imaginary dispersion curves can be seen in Figs. 3(a) and 3(b), respectively. By increasing \tilde{V}_0 , the amplitude of instability increases toward small wave numbers. A further increase in streaming velocity will help to stabilize the system. The effect of Z_d on the dispersion characteristics can be estimated in Figs. 4(a) and 4(b), which display, respectively, the value of real and imaginary parts of the normalized frequency. For high values of Z_d , the growth rate increases significantly toward small \tilde{k}_{\parallel} and with a further increase in Z_d , the growth rates tend to move toward large \tilde{k}_{\parallel} . The results indicate that even a small amount of dust charge is sufficient to modify the propagation and excitation of kinetic Alfvén-like instabilities.

The dust number density plays a significant role to study the above phenomenon. A sufficiently large amount of dust grains and for the beam velocity larger than the Alfvén velocity, we get two unstable solutions. One is the low frequency electromagnetic mode (kinetic Alfvén waves) coupled with Lorentzian and Doppler-shifted ion plasma oscillations in the beam resulting in the unstable branch and the other is near lower hybrid frequency; therefore, two separate unstable frequency bands may arise. The dispersion branches of KAW instability are shown in Fig. 5. It has been observed that the lower instability stabilizes due to the high concentration of the negatively charged dust grains, while the upper instability will increase for increased dust number density when $V_0 = 10$. For fixed plasma parameters, lower instability extends to short wavelength and large amplitude as compared to the upper instability.

From Figs. 6–10, we shall only discuss the upper instability.

Figure 6(a) shows real frequency as a function of \tilde{k}_{\parallel} . This figure indicates that the instability operates in the range $0.25 \leq \tilde{k}_{\parallel} \leq 0.42$ for $\kappa = 3$. In our case, $\tilde{k}_{\parallel} \sim 0.24$ ($\kappa \rightarrow \infty$) is the

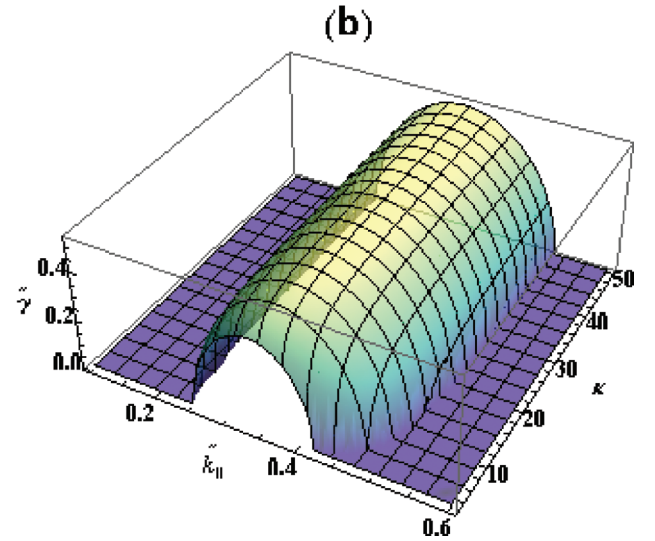
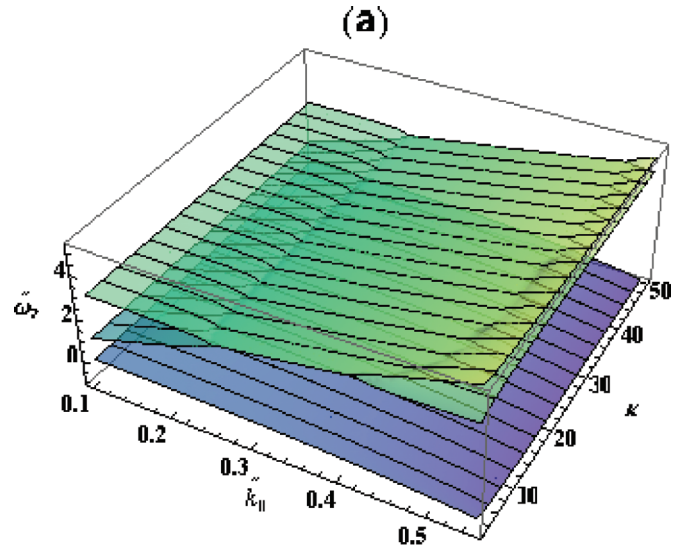


FIG. 6. (Color) Real ($\tilde{\omega}_r$) and imaginary ($\tilde{\gamma}$) parts as a function of \tilde{k}_{\parallel} and κ are plotted for $n_{d0} > 10^{-2}$, $\tilde{V}_0 = 10$, and $\beta_i = 0.6$.

critical value and for all other values before $\tilde{k}_{\parallel} = 0.24$, we arrive at a stable region. The superthermal feature appears to control the occurrence of instability, i.e., the instability is strongly modified. For small values of κ , the growth rate is reduced, but as we increase the value of κ , the growth rate enhances and eventually approaches its Maxwellian cousin as shown in the Fig. 6(b). Stable modes are also modified in the presence of nonthermality. Figure 7 shows that instability is strongly dependent on the β_i , i.e., it increases in amplitude; however, at the same time, the unstable region shifts toward large \tilde{k}_{\parallel} with the increase in β_i . It may be observed that the growth rates of unstable modes are reduced by increasing the non-neutrality parameter $\delta = n_{e0}/n_{i0}$ and by fixing $\beta_i \geq 0.5$, as depicted in Fig. 8. Since we assume the ions to drift with velocity \tilde{V}_0 due to ion current along magnetic field, the electromagnetic kinetic Alfvén-like wave will be unstable below electron cyclotron frequency, i.e., $\omega \ll \Omega_{ce}$. The free energy associated with the drift motion of ions is

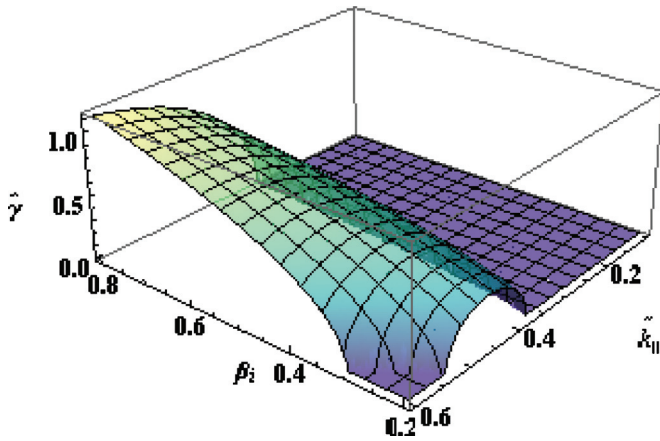


FIG. 7. (Color) Imaginary ($\tilde{\gamma}$) part as a function of \tilde{k}_{\parallel} and β_i is plotted for $n_{d0} > 10^{-2}$, $\tilde{V}_0 = 10$, and $\kappa = 3$.

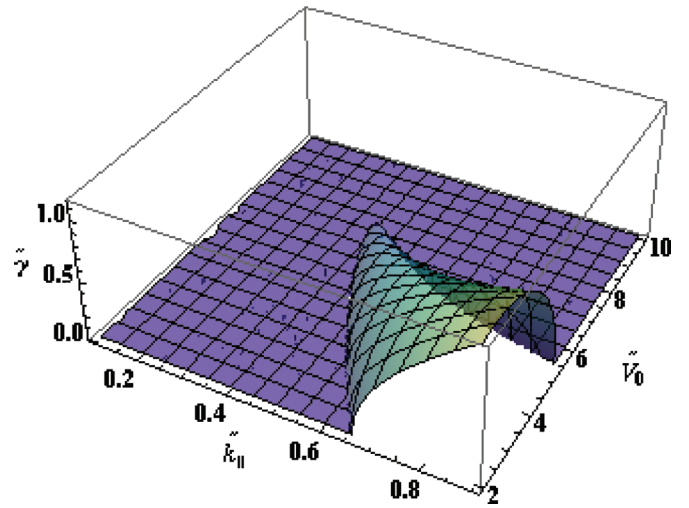


FIG. 9. (Color) Imaginary ($\tilde{\gamma}$) part as a function of \tilde{k}_{\parallel} and \tilde{V}_0 is plotted for $n_{d0} > 10^{-2}$, $\beta_i = 0.1$, and $\kappa = 3$.

responsible to excite the electromagnetic wave. The monotonically increasing trend of growth rates with the increase of flow velocity are presented in Fig. 9. It is shown that the instability increases with V_0 and a further increase will lead the mode toward stability. Thus, for a Lorentzian distribution, the wave frequency is lowered at higher ion beam velocities, which may be caused by the Doppler-shifting effects. Finally, we have observed the effect of charged dust grain on the electromagnetic wave instability. We can observe a rapid rise in the amplitude of unstable modes with the increase of charge on the dust grains as depicted in Fig. 10. It is obvious from our results that the presence of nonzero charge on the dust grain surface gives rise to a cutoff frequency at ω_{DLH} , which provides a limit for the propagation of an electromagnetic wave.

Waves and instabilities in molecular clouds have become outstanding and challenging topics in space science and modern astrophysics because of their vital role in understanding formation and evolution of interstellar molecular clouds containing dust grains.⁴⁹ The regions also having great amounts of dust particles can give rise to new wave modes or modify the pre-existing ones. It has also been

found earlier that there are some instances when molecules flourish in the presence of energetic radiation, high temperatures, and superthermal components of the molecular speed distribution.⁵⁰ Interstellar turbulence may allow the generation of Alfvén waves that propagate through the clouds in the direction of the magnetic field. The interactions of streaming instabilities with the background turbulence of interstellar medium may suppress the instabilities and cause damping of wave in a nonlinear regime.

Further, in the frame of *in situ* measurements, the proton velocity distribution functions has been observed in the solar wind, which show beam components,⁵¹ and the effect of dust grains on the instabilities of electromagnetic waves in the solar wind plasma due to ring beam cometary ion velocity distributions is well known in literature.⁵² On the other side, a number of investigations have been made to study the solar wind particle distribution function via kappa or generalized kappa distribution functions.^{34,53,54} Since the drift velocity of the beam relative to core protons is larger than the local

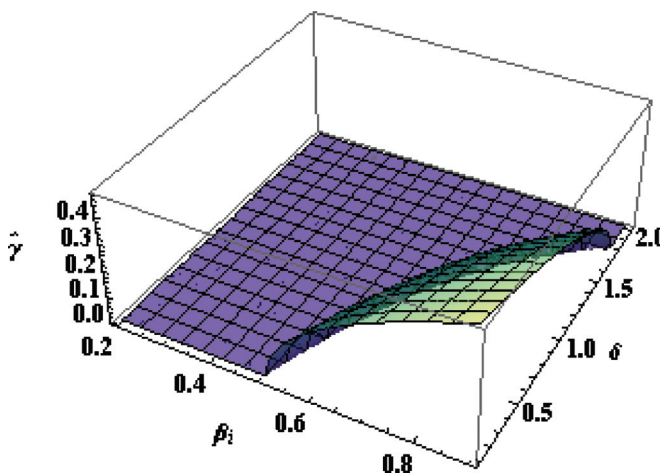


FIG. 8. (Color) Imaginary ($\tilde{\gamma}$) part as a function of β_i and δ is plotted for $n_{d0} > 10^{-2}$, $\tilde{V}_0 = 10$, $\tilde{k}_{\parallel} = 0.4$, and $\kappa = 3$.

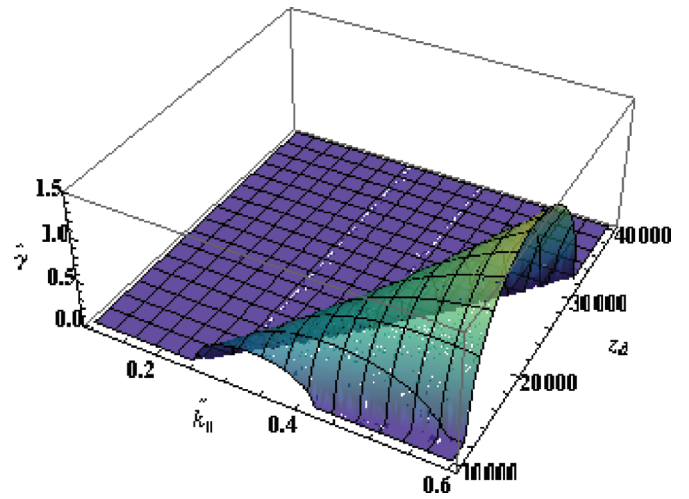


FIG. 10. (Color) Imaginary ($\tilde{\gamma}$) part as a function of \tilde{k}_{\parallel} and Z_d is plotted for $n_{d0} > 10^{-2}$, $\tilde{V}_0 = 10$, $\beta_i = 0.6$, and $\kappa = 3$.

Alfvén speed V_A , therefore, we may expect information about the solar coronal heating, solar wind acceleration, solar wind interaction with cometary dust, and the associated instabilities more accurately by using a Lorentzian distribution function.

In particular, the presented theory can also be applied to the solar wind, which contains numerous current sheets, e.g., heliospheric current sheet, and the belt of coronal streamers where the magnetic field orientation changes abruptly. The generally low speed ecliptic-plane wind also shows an abrupt switch to high-speed streams that originate from low-latitude coronal holes. In high-speed solar wind, the propagation of Alfvén waves can be transferred into fast magnetosonic waves. A penetration of dust from the interstellar origin to the vicinity of heliopause could have a significant effect on the wave properties

VI. CONCLUSIONS

In the present paper, we have analyzed the excitation of kinetic Alfvén-like streaming instabilities in a Lorentzian dusty plasma. Such type of instabilities are common in literature, but have not been investigated as far as a Lorentzian distribution is concerned. We have shown that κ -distributed ion beam with velocity \tilde{V}_0 passing through a background plasma having magnetized electrons and cold unmagnetized dust can excite kinetic Alfvén-type waves. The excited waves are normally shear Alfvén and dust acoustic modes. A general $\tilde{\omega}-\tilde{k}$ dispersion relation is derived in terms of a modified plasma dispersion function. We have obtained simple analytical forms of the dispersion relation by imposing different conditions. For parallel wave propagation ($\tilde{k}_\perp=0$), we get a longitudinal two stream instability in a dusty plasma and they are not influenced by the presence of external magnetic field. Similarly, for parallel wave propagation and $\tilde{V}_0=0$, we get whistler like waves in a dust free plasma when ($\omega_{ci} \ll \omega \ll \Omega_{ce}$). On the other hand in the limit $\omega/k_\parallel V_{Ae} \rightarrow 0$, we obtain linear dispersion relation of DAW. Our analytical investigations reveal that the presence of cold but mobile dust introduces a new cutoff frequency ω_{DLH} to KAW as compared to static dust which affects the dispersion of KAW through quasineutrality. It is found that the real frequency and the growth rates of this electromagnetic instability are significantly affected by the presence of a kappa distribution. The growth rates are reduced compared with a Maxwellian distribution. While the maximum growth rate tends to diminish, the instability extends to large waves numbers in the presence of superthermal particles. Instability tends to increase by the incremental variation of the streaming speed and the charge on the dust grain surface. Through coupling, the wave can take out the ions streaming energy to growing the amplitude of the mode. The impact of kappa distributed ions is found to be quite significant. We can also determine the ions superthermality spectral index, i.e., κ , when all other parameters are known. Dust number density plays an important role toward wave coupling and increasing drift velocity needed for the growth rates (upper instability). Higher dust concentrations will enhance the loss rate of electrons by attachment onto the dust grain which increases the

drift velocity and a further increase will lead toward stability and we can safely conclude that the reduction in the excitation of wave is expected.

The charging effects yield some additional currents which are the functions of streaming velocity, kappa, and some other electromagnetic effects due to magnetized electrons which require a separate detailed study and we also intend to pursue in the near future.

ACKNOWLEDGMENTS

This work is funded by the Higher Education Commission of Pakistan under the HEC-Overseas scholarship program Grant No. Ref: 1-1/PM OS /Phase-II/Batch-I/Austria/2007/. Part of this work was done while N. V. Erkaev was at the Space Research Institute of the Austrian Academy of Sciences in Graz. This work is also supported due to the RFBR Grant No. 09-05-91000-ANF-a. Further support is due to the ‘‘Austrian Fonds zur Förderung der Wissenschaftlichen Forschung’’ under Grant No. P20145-N16.

- ¹M. Lazar, *Phys. Lett. A* **372**, 2446 (2008).
- ²A. Bret, M.-C. Firpo, and C. Deutsch, *Laser Part. Beams* **24**, 27 (2006).
- ³M. R. Amin, A. M. Rizwan, M. K. Islam, M. Salimullah, and P. K. Shukla, *Phys. Scr.* **73**, 169 (2006).
- ⁴C. L. Chang, H. K. Wong, and C. S. Wu, *Phys. Rev. Lett.* **65**, 1104 (1990).
- ⁵D. Langmayr, H. K. Biernat, and N. V. Erkaev, *Phys. Plasmas* **12**, 102103 (2005).
- ⁶M. Rosenberg and N. A. Krall, *Planet. Space Sci.* **43**, 619 (1995).
- ⁷R. C. Tautz and R. Schlickeiser, *Phys. Plasmas* **12**, 122901 (2005).
- ⁸L. Gomberoff, G. Gnani, and F. T. Gratton, *J. Geophys. Res.* **101**, 13517, doi:10.1029/96JA00546 (1996).
- ⁹P. K. Shukla, *Astrophys. Space Sci.* **264**, 235 (1999).
- ¹⁰M. Rosenberg and P. K. Shukla, *J. Plasma Phys.* **70**, 317 (2004).
- ¹¹M. Salimullah, M. K. Islam, A. K. Banerjee, and M. Nambu, *Phys. Plasmas* **8**, 3510 (2001).
- ¹²S. Ali and P. K. Shukla, *Eur. Phys. J. D* **41**, 319 (2007).
- ¹³M. Salimullah, M. R. Amin, M. Salahuddin, and A. R. Chowdhury, *Phys. Scr.* **58**, 76 (1998).
- ¹⁴M. Salimullah and G. E. Morfill, *Phys. Rev. E* **59**, R2558 (1999).
- ¹⁵M. K. Islam, Y. Nakashima, K. Yatsu, and M. Salimullah, *Phys. Plasmas* **10**, 591 (2003).
- ¹⁶S. P. Gary, *Space Sci. Rev.* **56**, 373 (1991).
- ¹⁷R. Bharuthram, H. Saleem, and P. K. Shukla, *Phys. Scr.* **45**, 512 (1992).
- ¹⁸K. Sauer, E. Dubinin, and V. Tarasov, *Earth, Planets Space* **50**, 269 (1998).
- ¹⁹Y. Nariyuki, T. Hada, and K. Tsubouchi, *J. Geophys. Res.* **114**, A07102, doi:10.1029/2009JA014178 (2009).
- ²⁰M. C. de Juli, R. S. Schneider, L. F. Ziebell, and V. Jatenco-Pereira, *Phys. Plasmas* **12**, 052109 (2005).
- ²¹L. F. Ziebell, M. C. de Juli, R. S. Schneider, and V. Jatenco-Pereira, *Phys. Plasmas* **12**, 082102 (2005).
- ²²M. C. de Juli, R. S. Schneider, L. F. Ziebell, and R. Gaelzer, *J. Geophys. Res.* **112**, A10105, doi:10.1029/2007JA012434 (2007).
- ²³R. Gaelzer, M. C. de Juli, R. S. Schneider, and L. F. Ziebell, *Plasma Phys. Controlled Fusion* **51**, 015011 (2009).
- ²⁴N. S. Saini and I. Kourakis, *Phys. Plasmas* **15**, 123701 (2008).
- ²⁵V. M. Vasyliunas, *J. Geophys. Res.* **73**, 2839, doi:10.1029/JA073i009p02839 (1968).
- ²⁶S. P. Christon, D. Mitchell, D. Williams, L. Frank, C. Huang, and T. Eastman, *J. Geophys. Res.* **93**, 2562, doi:10.1029/JA093iA04p02562 (1988).
- ²⁷B. Abraham-Shrauner, J. R. Asbridge, S. J. Bame, and W. C. Feldman, *J. Geophys. Res.* **84**, 553, doi:10.1029/JA084iA02p00553 (1979).
- ²⁸M. P. Leubner, *J. Geophys. Res.* **87**, 6335, doi:10.1029/JA087iA08p06335 (1982).
- ²⁹S. Zaheer, G. Murtaza, and H. A. Shah, *Phys. Plasmas* **11**, 2246 (2004).
- ³⁰S. Zaheer, G. Murtaza, and H. A. Shah, *Phys. Plasmas* **13**, 062109 (2006).
- ³¹S. Zaheer, G. Murtaza, and H. A. Shah, *Phys. Plasmas* **14**, 022108 (2007).

- ³²N. Rubab and G. Murtaza, *Phys. Scr.* **73**, 178 (2006).
- ³³N. Rubab, G. Murtaza, and A. Mushtaq, *Phys. Plasmas* **13**, 112104 (2006).
- ³⁴Z. Kiran, H. A. Shah, M. N. S. Quershi, and G. Murtaza, *Sol. Phys.* **236**, 167 (2006).
- ³⁵F. Melandso, T. K. Aslaksen, and O. Havnes, *Planet. Space Sci.* **41**, 321 (1993).
- ³⁶A. Hasegawa and L. Chen, *Phys. Fluids* **19**, 1924 (1976).
- ³⁷K. Zubia, N. Rubab, H. A. Shah, M. Salimullah, and G. Murtaza, *Phys. Plasmas* **14**, 032105 (2007).
- ³⁸C. S. Liu and V. K. Tripathi, *Phys. Rep.* **130**, 143 (1986).
- ³⁹D. Summers and R. M. Thorne, *Phys. Fluids B* **3**, 1835 (1991).
- ⁴⁰C. E. J. Watt and R. Rankin, *J. Geophys. Res.* **112**, A04214, doi:10.1029/2006JA011907 (2007).
- ⁴¹N. Rubab, N. V. Erkaev, and H. K. Biernat, *Phys. Plasmas* **16**, 103704 (2009).
- ⁴²M. Lazar, R. Schlickeiser, S. Poedts, and R. C. Tautz, *Mon. Not. R. Astron. Soc.* **390**, 168 (2008).
- ⁴³*Basic Plasma Physics*, edited by A. A. Galeev and R. N. Sudan (North-Holland, Amsterdam, 1983).
- ⁴⁴H. Hasegawa, S. Irie, S. Usami, and Y. Ohsawa, *Phys. Plasmas* **9**, 2549 (2002).
- ⁴⁵M. J. Lee, *Phys. Plasmas* **14**, 032112 (2007).
- ⁴⁶Md. K. Alam, B. A. Begum, and A. R. Chowdhury, *Phys. Plasmas* **8**, 4318 (2001).
- ⁴⁷A. C. Das, A. K. Misra, and K. S. Goswami, *Phys. Rev. E* **53**, 4051 (1996).
- ⁴⁸S. A. Shan, H. Saleem, and M. Sajid, *Phys. Plasmas* **15**, 072904 (2008).
- ⁴⁹A. A. Mamun and P. K. Shukla, *JETP Lett.* **75**, 213 (2002).
- ⁵⁰H. J. Black, *Faraday Discuss.* **109**, 257 (1998).
- ⁵¹E. Marsch, *Living Rev. Sol. Phys.* **3**, 1 (2006).
- ⁵²N. F. Cramer, F. Verheest, and S. V. Vladimirov, *Phys. Plasmas* **6**, 36 (1999).
- ⁵³M. N. S. Qureshi, G. Pallochia, R. Bruno, M. B. Cattaneo, V. Formisano, H. A. Shah, H. Reme, J. M. Bosued, I. Dandouras, J. A. Sauvaud, L. Kistler, E. Moebius, B. Klecker, C. W. Carlson, J. P. McFadden, G. K. Parks, M. McCarthy, A. Korth, R. Lundin, and A. Balogh, *AIP Conf. Proc.* **679**, 489 (2003).
- ⁵⁴M. Maksimovic, V. Pierrard, and J. F. Lemaire, *Astron. Astrophys.* **324**, 725 (1997).